Mixed-Chalcogenide, Mixed-Metal Carbonyl Clusters. Synthesis and Characterization of $Cp_2Mo_2Fe_2(\mu_4\text{-Te})(\mu_3\text{-E})(\mu_3\text{-E}')(CO)_6$ (E, E′ = Te; E = S, E′ = Te; E, E′ = S; E = S, E′ = Se), $Cp_2Mo_2Fe_2(\mu_3\text{-Te})(\mu_3\text{-E})(CO)_7$, and $Cp_2Mo_2Fe(\mu_3\text{-E})(CO)_7$ (E = S, Te)

Pradeep Mathur,* Md. Munkir Hossain, and Shubhangi B. Umbarkar

Chemistry Department, Indian Institute of Technology, Bombay 400 076, India

C. V. V. Satyanarayana

Regional Sophisticated Instrumentation Center, Indian Institute of Technology, Powai, Bombay 400 076, India

Arnold L. Rheingold,* Louise M. Liable-Sands, and Glenn P. A. Yap

Department of Chemistry, University of Delaware, Newark, Delaware 19716

Received November 7, 1995[⊗]

Reflux of a benzene solution of $Fe_3STe(CO)_9$ and $Cp_2Mo_2(CO)_6$ yielded the new cluster $Cp_2Mo_2Fe_2STe(CO)_7$ (**6**) as the major product and the following clusters in smaller amounts: $Cp_2Mo_2Fe_2Te_3(CO)_6$ (**1**), $Cp_2Mo_2Fe_2STe_2(CO)_6$ (**2**), $Cp_2Mo_2Fe_2S_2Te(CO)_6$ (**3**), $Cp_2Mo_2FeTe(CO)_7$ (**4**), $Cp_2Mo_2FeS(CO)_7$ (**5**), and $Cp_2Mo_2Fe_2Te_2(CO)_7$ (**7**). The new cluster **3** was formed in good yield when a benzene solution of **6** was refluxed with sulfur powder. Similarly, **2** was obtained when a benzene solution of **6** was refluxed with tellurium powder. A new cluster with three different chalcogen ligands, $Cp_2Mo_2Fe_2SSeTe(CO)_6$ (**8**), was obtained when a benzene solution of **6** was refluxed in the presence of selenium powder. Structures of **1**−**4**, **6**, and **8** were established by crystallographic methods. The structures of **1**−**3** and **8** consist of Mo_2Fe_2 butterfly cores with a μ_4-Te atom and two μ_3-chalcogen atoms (**1**, Te and Te; **2**, S and Te; **3**, S and S; **8**, S and Se) capping the two Mo_2Fe faces. Each Mo atom has a Cp ligand, and each Fe atom has three terminally bonded carbonyl groups. The structure of **4** conists of a Mo_2FeTe tetrahedron with each Mo possessing a Cp ligand and two terminally bonded carbonyl groups and the Fe atom having three terminal carbonyl groups attached to it. The structure of **6** consists of a Mo_2Fe_2 tetrahedron. One Mo_2Fe face is capped by a μ_3-S ligand and the other by a μ_3-Te atom. The Fe−Fe bond is bridged by a carbonyl group; there are two terminally bonded carbonyl groups attached to each Fe atom. A semitriply bridging carbonyl group is attached to one Mo atom. The other Mo atom has one terminal carbonyl group. Each Mo atom has one Cp ligand attached to it.

Introduction

There has been continuing interest in chalcogen-bridged transition-metal carbonyl clusters,[1] and there are several methods available for the incorporation of chalcogen atoms in metal complexes.[2] The classes of compounds $Fe_3(CO)_9(\mu_3\text{-}E_2)$ and $Fe_2(CO)_6(\mu\text{-}E_2)$ (E = S, Se, Te) have been shown to be good starting materials for obtaining chalcogen-bridged clusters.[3] Reduction of Na_2EO_3 with $[HFe(CO)_4]^-$ is a convenient route for preparing $Fe_3(CO)_9(\mu_3\text{-}E)_2$, which can be converted into the more reactive $Fe_2(CO)_6(\mu\text{-}E_2)$ on treatment with NaOMe followed by acidification.[4] An attractive feature of the use of these reagents is that they undergo cluster growth reactions under mild conditions, often at room temperature. Also, their reactions have been shown to be dependent on the nature of E. Rauchfuss and co-workers have reported on the contrast in reactivity of $Fe_3(CO)_9(\mu_3\text{-Te})_2$ with that of $Fe_3(CO)_9(\mu_3\text{-S})_2$ and $Fe_3(CO)_9(\mu_3\text{-Se})_2$ toward a variety of Lewis bases; whereas the Te_2 compound can form Lewis base adducts of the

[⊗] Abstract published in *Advance ACS Abstracts,* March 1, 1996.

(1) (a) Roof, L. C.; Kolis, J. W. *Chem. Rev.* **1993**, *93*, 1037. (b) Wachter, J. *Angew, Chem., Int. Ed. Engl.* **1989**, *28*, 1613. (c) Muller, A. *Polyhedron* **1986**, *5*, 323. (d) Wachter, J. *J. Coord. Chem.* **1988**, *15*, 219. (e) Whitmire, J. *J. Coord. Chem.* **1988**, *17*, 95. (f) Ansari, M. A.; Ibers, J. A. *Coord. Chem. Rev.* **1990**, *100*, 223. (g) Tatsumi, K.; Kawaguchi, H.; Tani, K. *Angew. Chem. Int. Ed. Engl.* **1993**, *32*, 591. (h) Linford, L.; Raubenheimer, H. G. *Adv. Organomet. Chem.* **1991**, *32*, 1. (i) Compton, N. A.; Errington, R. J.; Norman, N. C. *Adv. Organomet. Chem.* **1990**, *31*, 91.

(2) (a) Flomer, W. A.; O'Neal, S. C.; Kolis, J. W.; Jeter, D.; Cordes, A. W. *Inorg. Chem.* **1988**, *27*, 969. (b) O'Neal, S. C.; Pennington, W. T.; Kolis, J. W. *Can. J. Chem.* **1989**, *67*, 1980. (c) O'Neal, S. C.; Pennington, W. T.; Kolis, J. W. *Inorg. Chem.* **1990**, *29*, 3134. (d) Roof, L. C.; Pennington, W. T.; Kolis, J. W. *J. Am. Chem. Soc.* **1990**, *112*, 8172. (e) Kolis, J. W. *Coord. Chem. Rev.* **1990**, *105*, 195. (f) Roof, L. C.; Pennington, W. T.; Kolis, J. W. *Angew. Chem., Int. Ed. Engl.* **1992**, *31*, 913. (g) Dranganjac, M.; Dhingra, S.; Huang, S. P.; Kanatzidis, M. G. *Inorg. Chem.* **1990**, *29*, 590.

(3) Mathur, P.; Chakrabarty, D.; Mavunkal, I. J. *J. Cluster Sci.* **1993**, *4*, 351.

(4) (a) Bogan, L. E.; Lesch, D. A.; Rauchfuss, T. B. *J. Organomet. Chem.* **1983**, *250*, 429. (b) Mathur, P.; Chakrabarty, D.; Hossain, M. M.; Rashid, R. S.; Rugmini, V.; Rheingold, A. L. *Inorg. Chem.* **1992**, *31*, 1106.

0276-7333/96/2315-1898$12.00/0

form $Fe_2(CO)_6(\mu_3\text{-}Te)_2Fe(CO)_3L$, the S_2 and the Se_2 compounds do not form the corresponding adducts.[5] Differences in reactivity of $Fe_2(CO)_6(\mu\text{-}E_2)$ for different E ligands are exemplified by the reaction of $Fe_2(CO)_6(\mu\text{-}Se_2)$ with phenylacetylene to form $(CO)_6Fe_2\{\mu\text{-}SeC(Ph)=C(H)Se\}$.[6] The S_2 and Te_2 compounds show no reactivity towards phenylacetylene under similar conditions. The compounds $(CO)_6Fe_2\{\mu\text{-}SC(Ph)=C(H)S\}$[7] and $(CO)_6Fe_2\{\mu\text{-}TeC(Ph)=C(H)Te\}$[8] have been obtained by different routes. Addition of mononuclear metal carbonyl groups takes place readily in a stepwise manner to give trinuclear clusters $Fe_2M(CO)_9(\mu_3\text{-}E)_2$ and tetranuclear clusters $Fe_2M_2(CO)_9(\mu_4\text{-}E)_2$ (M = Fe, Ru).[3,9] Availability of the mixed-chalcogenide compounds $Fe_3(CO)_9(\mu_3\text{-}E)(\mu_3\text{-}E')$ and $Fe_2(CO)_6(\mu\text{-}EE')$ ($E \neq E'$, E, E' = S, Se, Te)[10] by convenient synthetic routes now gives us an opportunity to introduce a greater variety to the composition of clusters of a particular structural type. The reaction of $Fe_2(CO)_6(\mu\text{-}S_2)$ with $Cp_2Mo_2(CO)_4$ is reported to form the cis-"Braunstein" and trans-"Curtis" isomers of $Cp_2Mo_2Fe_2S_2(CO)_8$.[11] On the other hand, $Fe_2(CO)_6(\mu\text{-}Se_2)$ reacts with $Cp_2Mo_2(CO)_4$ to form $Cp_2Mo_2Fe_2(\mu_4\text{-}Se)(\mu_3\text{-}Se)_2(CO)_6$ and $Cp_2Mo_2Fe_2(\mu_3\text{-}Se)_2(CO)_7$.[12] Here we report on the thermolysis of the mixed chalcogenide $Fe_3(CO)_9(\mu_3\text{-}S)(\mu_3\text{-}Te)$ with $Cp_2Mo_2(CO)_6$ and the formation of new mixed Fe/Mo, mixed-chalcogenide clusters.

Experimental Section

General Procedures. All reactions and other manipulations were performed using standard Schlenk techniques under an inert atmosphere of argon. All solvents were deoxygenated immediately prior to use. Infrared spectra were recorded on a Nicolet 5DXB or Impact 400 FTIR spectrophotometer as hexane or dichloromethane solutions in 0.1 mm pathlength NaCl cells. Elemental analyses were performed using a Carlo Erba automatic analyzer. ^1H, ^{13}C, ^{77}Se, and ^{125}Te NMR spectra were recorded on a Varian VXR-300S spectrometer in $CDCl_3$. The operating frequency for ^{77}Se NMR was 57.23 MHz, with a pulse width of 15 μs and a delay of 1 s. The operating frequency for ^{125}Te NMR was 94.705 MHz with a pulse width of 9.5 μs and a delay of 1 s. ^{77}Se NMR spectra are referenced to Me_2Se (δ 0), and ^{125}Te NMR spectra are referenced to Me_2Te (δ 0). $Fe_3STe(CO)_9$,[9b] $Fe_2STe(CO)_6$,[9b] $Fe_3Te_2(CO)_9$,[13] and $Cp_2Mo_2(CO)_6$[14] were prepared as previously reported.

Reaction of $Fe_3STe(CO)_9$ with $Cp_2Mo_2(CO)_6$. A benzene solution (100 mL) of $Fe_3STe(CO)_9$ (0.4 g, 0.88 mmol) and $Cp_2Mo_2(CO)_6$ (0.3 g, 0.61 mmol) was refluxed for 40 h. The solvent was removed *in vacuo*, and the residue was subjected to chromatographic workup. Using a hexane/dichloromethane (50/50 v/v) mixture as eluent, three fractions were collected, each of which was subjected to further chromatographic workup on silica gel TLC plates. Chromatography of the first band, using a hexane/dichloromethane (70/30 v/v) mixture as eluent, yielded the following three compounds, in order of elution: dark red $Cp_2Mo_2Fe_2Te_3(CO)_6$ (**1**; 30 mg, 5%), dark red $Cp_2Mo_2Fe_2STe_2(CO)_6$ (**2**; 92 mg, 17%), and deep red $Cp_2Mo_2Fe_2S_2Te(CO)_6$ (**3**; 34 mg, 7%). Chromatography of the second band, using a hexane/dichloromethane (50/50 v/v) mixture, separated two dark red bands, in order of elution: $Cp_2Mo_2FeTe(CO)_7$ (**4**; 13 mg, 3%) and $Cp_2Mo_2FeS(CO)_7$ (**5**; 22 mg, 6%). Chromatography of the third band, using a hexane/dichloromethane (40/60 v/v) mixture, separated the following two black compounds, in order of elution: $Cp_2Mo_2Fe_2STe(CO)_7$ (**6**; 149 mg, 31%) and $Cp_2Mo_2Fe_2Te_2(CO)_7$ (**7**; 16 mg, 3%). **1**: mp 210−211 °C. Anal. Calcd (found) for $C_{16}H_{10}Fe_2Mo_2O_6Te_3$: C, 19.5 (19.7); H 1.02 (1.07). **2**: mp 198−199 °C. Anal. Calcd (found) for $C_{16}H_{10}Fe_2Mo_2O_6STe_2$: C, 21.6 (21.4); H, 1.12 (1.33). **3**: mp 158−159 °C. Anal. Calcd (found) for $C_{16}H_{10}Fe_2Mo_2O_6S_2Te$: C, 24.2 (24.3); H, 1.26 (1.33). **4**: mp 157−158 °C. Anal. Calcd (found) for $C_{17}H_{10}FeMo_2O_7Te$: C, 29.1 (29.2); H, 1.42 (1.52). **5**: mp 142−143 °C. Anal. Calcd (found) for $C_{17}H_{10}Fe_2Mo_2O_7S$: C, 33.7 (33.5); H, 1.65 (1.72). **6**: mp 139−140 °C. Anal. Calcd (found) for $C_{17}H_{10}Fe_2Mo_2O_7STe$: C, 25.8 (25.7); H, 1.27 (1.37). **7**: mp 118−119 °C. Anal. Calcd (found) for $C_{17}H_{10}Fe_2Mo_2O_7Te_2$: C, 23.1 (23.1); H, 1.13 (1.23).

Reaction of Sulfur Powder with 6. A benzene solution (50 mL) of **6** (157 mg, 0.2 mmol) and sulfur powder (13 mg, 0.4 mmol) was refluxed for 10 h. The reaction mixture was filtered through Celite to remove unreacted sulfur powder. Chromatographic workup on silica gel TLC plates with a hexane/dichloromethane (70/30 v/v) mixture yielded the following, in order of elution: a major red band of **3** (81 mg, 51%) and a trace amount of unreacted **6**.

Reaction of Tellurium Powder with 6. A benzene solution (50 mL) of **6** (157 mg, 0.2 mmol) and tellurium powder (38 mg, 0.3 mmol) was refluxed for 9 h. The reaction mixture was filtered through Celite to remove unreacted tellurium powder. Chromatographic workup on silica gel TLC plates with a hexane/dichloromethane (70/30 v/v) mixture yielded two major products, in order of elution: **2** (29 mg, 11%) and **3** (74 mg, 31%), followed by a trace amount of **6**.

Reaction of Selenium Powder with 6. A benzene solution (50 mL) of **6** (157 mg, 0.2 mmol) and selenium powder (23 mg, 0.3 mmol) was refluxed for 6 h. The reaction mixture was filtered through Celite to remove unreacted selenium powder. Chromatographic workup on silica gel TLC plates with a hexane/dichloromethane (70/30 v/v) mixture separated the major black band of $Cp_2Mo_2Fe_2SSeTe(CO)_6$ (**8**) (105 mg, 63%) from a trace amount of unreacted **6**. **8**: mp 168−169 °C. Anal. Calcd (found) for $C_{16}H_{10}Fe_2Mo_2O_6SSeTe$: C, 22.8 (22.7); H, 1.19 (1.21).

Crystal Structure Determination of 1−4, 6, and 8. Crystal data collection and refinement parameters are given in Table 1. Suitable crystals were selected and mounted with epoxy cement on glass fibers. The unit-cell parameters were obtained by least-squares refinement of the angular settings of 24 reflections ($20° \leq 2\theta \leq 24°$).

The photographic data, unit-cell parameters, occurrence of equivalent reflections, and systematic absences in the diffraction data are consistent with $Pna2_1$ or $Pnam$ ($Pnma$) for **6**, $P\bar{1}$ or $P1$ for **4**, Cm or $C2/m$ for **2**, $Imm2$, $Immm$, $I222$, or $I2_12_12_1$ for **1**, and uniquely $P2_1/n$ for both **8** and **3**. The E statistics suggested the noncentrosymmetric options for **6** and **1** and the centrosymmetric options for **2** and **4**. The occupancy ($Z = 2$) of **1** eliminated the space group $I2_12_12_1$, while the molecular symmetry strongly suggested $Imm2$. The space group choices were confirmed by chemically reasonable results of refinement.

The structures were solved by using direct methods, completed by difference Fourier syntheses, and refined by full-matrix least-squares procedures. Semi-empirical absorption corrections were applied. The cyclopentadienyl carbon atoms

(5) Lesch, D. A.; Rauchfuss, T. B. *Organometallics* **1982**, *1*, 499.
(6) Mathur, P.; Hossain, M. M. *Organometallics* **1993**, *12*, 2398. (b) Mathur, P.; Hossain, M. M.; Das, K.; Sinha, U. C. *J. Chem. Soc., Chem. Commun.* **1992**, 46.
(7) Seyferth, D.; Womack, G. B. *Organometallics* **1986**, *5*, 2360.
(8) Fassler, T.; Buchholz, D.; Huttner, G.; Zsolnai, L. *J. Organomet. Chem.* **1989**, *369*, 297.
(9) (a) Mathur, P.; Hossain, M. M.; Rashid, R. S. *J. Organomet. Chem.* **1993**, *460*, 83. (b) Mathur, P.; Chakrabarty, D.; Hossain, M. M. *J. Organomet. Chem.* **1991**, *418*, 415.
(10) (a) Mathur, P.; Sekar, P.; Satyanarayana, C. V. V.; Mahon, M. F. *Organometallics* **1995**, *14*, 2115. (b) Mathur, P.; Hossain, M. M.; Umbarkar, S.; Satyanarayana, C. V. V.; Tavale, S. S.; Puranik, V. G. *Organometallics* **1995**, *14*, 959. (c) Mathur, P.; Chakrabarty, D.; Hossain, M. M. *J. Organomet. Chem.* **1991**, *401*, 167.
(11) (a) Braunstein, P.; Jud, J.-M.; Tiripicchio-Camellini, M.; Sappa, E. *Angew. Chem., Int. Ed. Engl.* **1982**, *21*, 307. (b) Williams, P. D.; Curtis, M. D.; Duffy, D. N.; Butler, W. D. *Organometallics* **1983**, *2*, 165.
(12) Mathur, P.; Hossain, M. M.; Rheingold, A. L. *Organometallics* **1994**, *13*, 3909.
(13) Lesch, D. A.; Rauchfuss, T. B. *Inorg. Chem.* **1981**, *20*, 3583.
(14) Ginley, D. S.; Bock, C. R.; Wrighton, M. S. *Inorg. Chim. Acta* **1977**, *23*, 85.

Table 1. Crystallographic Data for 1−4, 6, and 8

	1	2	3	4	6	8
			(a) Crystal Parameters			
formula	$C_{16}H_{10}O_6Fe_2Mo_2Te_3$	$C_{16}H_{10}O_6Fe_2Mo_2STe_2$	$C_{16}H_{10}O_6Fe_2Mo_2S_2Te$	$C_{17}H_{10}O_7FeMo_2Te$	$C_{17}H_{10}O_7SFe_2Mo_2Te$	$C_{16}H_{10}O_6Fe_2Mo_2SSeTe$
fw	984.62	889.08	793.5	701.6	787.1	838.4
cryst syst	orthorhombic	monoclinic	monoclinic	triclinic	orthorhombic	monoclinic
space group	$Imm2$	$C2/m$	$P2_1/n$	$P\bar{1}$	$Pna2_1$	$P2_1/n$
a, Å	10.385(1)	16.647(5)	10.498(3)	7.904(2)	13.524(4)	10.454(5)
b, Å	14.545(3)	10.200(3)	35.507(8)	8.186(2)	12.843(4)	35.484(6)
c, Å	7.130(1)	12.963(5)	12.347(2)	16.401(8)	11.989(4)	12.393(5)
α, deg				83.21(3)		
β, deg		102.54(3)	112.99(2)	78.15(3)		112.86(2)
γ, deg				68.70(2)		
V, Å^3	1077.01(25)	2148.6(12)	4237(1)	966.5(6)	2082.9(11)	4236(3)
Z	2	4	8	2	4	8
cryst dimens, mm	0.30 × 0.30 × 0.30	0.25 × 0.30 × 0.40	0.16 × 0.18 × 0.42	0.30 × 0.40 × 0.40	0.20 × 0.28 × 0.37	0.40 × 0.40 × 0.54
cryst color	dark red	dark red	deep red	dark red	black	black
D(calc), g cm^{-3}	3.036	2.748	2.488	2.411	2.510	2.619
μ(Mo Kα), cm^{-1}	64.71	52.53	40.76	35.35	39.04	56.74
temp, K	296	255	296	255	245	296
			(b) Data Collection			
diffractometer			Siemens P4			
monochromator			graphite			
radiation			Mo Kα (λ = 0.710 73 Å)			
2θ scan range, deg	4−65	4−60	4−60	4−45	4−48	4−50
no. of rflns collected	1472	3085	11169	2631	2137	8128
no. of indpt rflns	1277	2980	10769	2527	1945	7844
no. of indpt obsd rflns ($F_o \geq n\sigma(F_o)$)	1217 (n = 4)	2162 (n = 4)	7209 (n = 4)	2391 (n = 4)	1921 (n = 4)	6111 (n = 5)
			(c) Refinement			
$R(F)$, %	3.12[b]	5.85[b]	6.54[a]	2.15[a]	3.00[a]	7.67[a]
$R_w(F)$, %	7.48[b,c]	14.34[b,c]	9.58[a]	3.53[a]	4.99[a]	11.05[a]
Δ/σ (max)	0.002	0.001	0.569	0.002	0.004	0.064
$\Delta(\rho)$, e Å^{-3}	1.325	1.250	1.50	0.43	1.08	2.68
N_o/N_v	16.4	20.4	14.8	9.5	7.6	15.8
GOF	1.088	1.00	1.18	1.00	1.50	1.51

[a] Quantity minimized $\sum w\Delta^2$; $R = \sum\Delta/\sum(F_o)$; $R_w = \sum\Delta w^{1/2}/\sum(F_o w^{1/2})$, $\Delta = |F_o = F_c|$. [b] Quantity minimized $\sum[w(F_o^2 - F_c)^2]^2/\sum[(wF_o^2)^2]^{1/2}$; $R = \sum\Delta/\sum(F_o)$; $R_w = \sum\Delta w^{1/2}/\sum(F_o w^{1/2})$, $\Delta = |(F_o - F_c)|$. [c] $R_w(F^2)$, %.

Table 2. Selected Bond Lengths (Å) and Bond Angles (deg) for 1

Te(1)−Fe	2.7087(12)	Te(1)−Mo	2.6369(9)
Te(2)−Fe	2.5124(14)	Te(2)−Mo	2.6639(7)
Mo−Fe	2.9357(11)	Mo−Mo(A)	2.8172(12)
Mo(A)−Te(1)−Mo	64.58(3)	Mo−Te(1)−Fe	66.61(2)
Te(1)−Mo−Te(2A)	113.0(3)	Mo(A)−Te(2)−Mo	63.85(3)
Te(2A)−Mo−Te(2)	80.57(3)	Te(1)−Mo−Mo(A)	57.71(2)
Te(2)−Mo−Mo(A)	58.077(14)	Te(1)−Mo−Fe	57.87(3)
Te(2)−Mo−Fe	53.05(3)	Te(2A)−Mo−Fe(A)	53.05(3)
Te(1)−Fe−Mo(A)	55.53(3)	Mo(A)−Te(1)−Fe	66.61(2)
Fe−Te(1)−Fe(A)	123.97(6)	Fe−Te(2)−Mo	69.03(3)
Te(2A)−Mo−Fe	116.88(3)	Mo(A)−Mo−Fe	61.33(2)
Te(1)−Mo−Fe(A)	57.87(3)	Fe−Mo−Fe(A)	109.09(4)
Te(2)−Fe−Te(1)	102.57(4)	Te(2)−Fe−Mo	57.92(3)
Mo(A)−Fe−Mo	57.35(3)	Te(1)−Fe−Mo	55.53(3)

in **8** and **3** were refined isotropically and as rigid rings. All other non-hydrogen atoms were refined with anisotropic displacement coefficients. Hydrogen atoms were treated as idealized contributions.

The isomorphous structures **8** and **3** have two independent, but chemically equivalent, molecules in the asymmetric unit. The tricoordinated chalcogen atoms in **6** and **8** were found to be statistically disordered between two positions with a distribution of 77/23 in **6** and 50/50 in **8**. This disorder was modeled by refining the occupancies of the chalcogen atoms which were identified as the major contributor in **6** and arbitrarily as selenium in **8** (labeled as Ss(1), Ss(2), Ss(1′) and Ss(2′)). The largest remaining peaks in the difference maps (1.1−2.7 e Å^{-3}) occur at chemically unreasonable positions and were considered as noise. Tables 2−7 list selected bond lengths and bond angles, respectively, for **1**−**4**, **6**, and **8**. For both structures **1** and **6**, the correct enantiomorph was determined unambiguously by the Rogers test.

All software and sources of the scattering factors are contained in either the SHELXTL PLUS (4.2) or SHELXTL (5.1) program libraries (G. Sheldrick, Siemens XRD, Madison, WI).

Results and Discussion

Synthesis. When a benzene solution containing $(CO)_9Fe_3(\mu_3\text{-}S)(\mu_3\text{-}Te)$ and $Cp_2Mo_2(CO)_6$ was refluxed for 40 h, the new mixed-metal, mixed-chalcogenide cluster $Cp_2Mo_2Fe_2(CO)_7(\mu_3\text{-}S)(\mu_3\text{-}Te)$ (**6**; 31%) was obtained as the major product. In addition, the following clusters were also isolated from the reaction: $Cp_2Mo_2Fe_2(CO)_6(\mu_3\text{-}Te)_2(\mu_4\text{-}Te)$ (**1**; 5%), $Cp_2Mo_2Fe_2(CO)_6(\mu_3\text{-}S)(\mu_3\text{-}Te)(\mu_4\text{-}Te)$ (**2**; 17%), $Cp_2Mo_2Fe_2(CO)_6(\mu_3\text{-}S)_2(\mu_4\text{-}Te)$ (**3**; 7%), $Cp_2Mo_2Fe(CO)_7(\mu_3\text{-}Te)$ (**4**; 3%), $Cp_2Mo_2Fe(CO)_7(\mu_3\text{-}S)$ (**5**; 6%), and $Cp_2Mo_2Fe_2(CO)_7(\mu_3\text{-}Te)_2$ (**7**; 3%) (Scheme 1). Compound **3** was isolated in 51% yield when a benzene solution of **6** and sulfur powder was refluxed for 10 h (Scheme 2). When a benzene solution of **6** was refluxed for **9** h in the presence of tellurium powder, **2** (11%) and **3** (31%) were formed. Use of a large excess of tellurium powder did not lead to an improved yield of **2**. Since significant amounts of **3** are also formed during the reaction, a certain amount of cluster degradation must occur to make available free S, which then reacts with **6** to form cluster **3**. A novel cluster with three different chalcogen ligands, $Cp_2Mo_2Fe_2(CO)_6(\mu_3\text{-}S)(\mu_3\text{-}Se)(\mu_4\text{-}Te)$ (**8**), was isolated in 63% yield from the benzene reflux for 6 h of **6** in the presence of selenium powder (Scheme 3). The Te_3 cluster **1** was obtained in a slightly improved yield (14%) from the benzene reflux reaction

Scheme 1

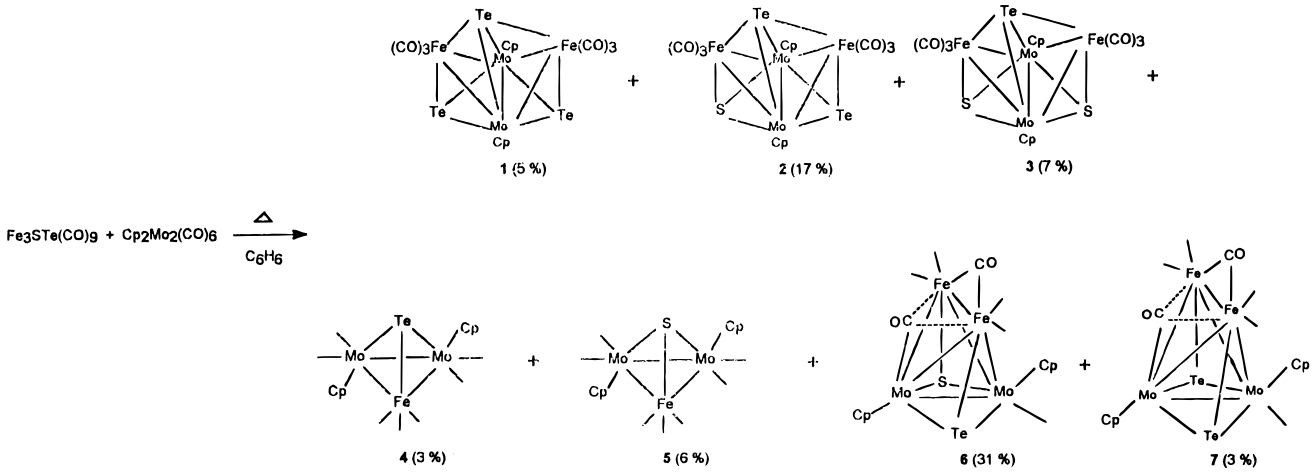

Table 3. Selected Bond Lengths (Å) and Bond Angles (deg) for 2

Te(1)−Mo(1)	2.6153(10)	Te(1)−Fe(1)	2.668(2)
Te(2)−Fe(1)	2.521(2)	Mo(1)−S(1)	2.404(2)
Mo(1)−Fe(2)	2.854(2)	Te(1)−Fe(2)	2.849(2)
Te(2)−Mo(1)	2.6630(10)	Mo(1)−Mo(1A)	2.7510(13)
Mo(1)−Fe(1)	2.905(2)	Fe(2)−S(1)	2.224(3)

Mo(1)−Te(1)−Mo(1A)	63.46(4)	Mo(1A)−Te(1)−Fe(1)	66.70(4)
Mo(1A)−Te(1)−Fe(2)	62.81(4)	Fe(1)−Te(2)−Mo(1)	68.10(4)
Mo(1)−Te(2)−Mo(1A)	62.20(3)	Te(1)−Mo(1)−Te(2)	101.27(3)
S(1)−Mo(1)−Mo(1A)	55.10(4)	Te(2)−Mo(1)−Mo(1A)	58.90(2)
Te(2)−Mo(1)−Fe(2)	115.96(3)	Te(1)−Mo(1)−Fe(1)	57.52(4)
Mo(1A)−Mo(1)−Fe(1)	61.74(2)	Mo(1)−Te(1)−Fe(1)	66.70(4)
Mo(1)−Te(1)−Fe(2)	62.81(4)	Fe(1)−Te(1)−Fe(2)	119.80(5)
Fe(1)−Te(2)−Mo(1A)	62.20(4)	S(1)−Mo(1)−Te(1)	99.59(5)
S(1)−Mo(1)−Te(2)	78.60(6)	Te(1)−Mo(1)−Mo(1A)	58.27(2)
Te(1)−Mo(1)−Fe(2)	62.59(4)	Mo(1A)−Mo(1)−Fe(2)	61.19(2)
S(1)−Mo(1)−Fe(1)	114.21(5)	Te(2)−Mo(1)−Fe(1)	53.63(4)
Fe(2)−Mo(1)−Fe(1)	111.96(4)	Te(1)−Fe(1)−Mo(1)	55.78(4)
Te(2)−Fe(1)−Mo(1A)	58.27(4)	Mo(1)−Fe(1)−Mo(1A)	56.52(4)
S(1)−Fe(2)−Te(1)	97.50(9)	S(1)−Fe(2)−Mo(1A)	54.82(6)
Te(1)−Fe(2)−Mo(1)	54.59(4)	Fe(2)−S(1)−Mo(1A)	76.04(8)
Mo(1A)−S(1)−Mo(1)	69.81(7)	Te(2)−Fe(1)−Te(1)	103.65(6)
Te(2)−Fe(1)−Mo(1)	58.27(4)	Te(1)−Fe(1)−Mo(1A)	55.78(4)
Te(1)−Fe(2)−Mo(1A)	54.59(4)	S(1)−Fe(2)−Mo(1)	54.82(6)
Mo(1A)−Fe(2)−Mo(1)	57.62(4)	Fe(2)−S(1)−Mo(1)	76.04(8)

Scheme 2

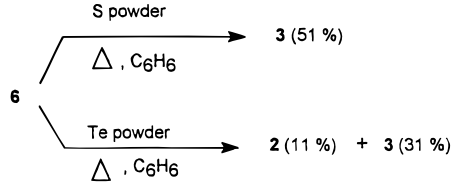

Scheme 3

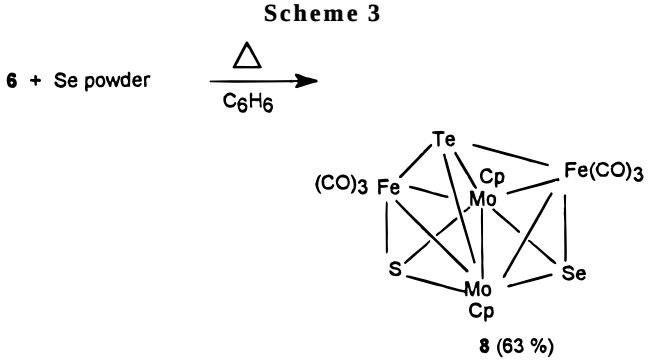

of $Cp_2Mo_2(CO)_6$ and $Fe_3(CO)_9(\mu_3\text{-}Te)_2$. Also formed in this reaction were **4** in 17% yield and **7** in 23% yield.

Spectroscopic Characterization. Clusters **1**−**8** were characterized by IR and NMR spectroscopy (Table 8). Identification of **1**, **4**, **5**, and **7** was made by comparison of IR and ^{1}H NMR data with those reported. Rauchfuss has reported that **1** and **4** are formed as minor products from the reaction of $Cp_2Mo_2(CO)_6$ and $Fe_3(CO)_9(\mu_3\text{-}Te)_2$ at high temperature and high CO pressure. This reaction produces $Cp_2Mo_2FeTe_2(CO)_7$ as the major product, which on thermolysis yields compound **7**, in addition to **1** and **4**, and the X-ray structure

Table 4. Selected Bond Lengths (Å) and Bond Angles (deg) for 3

Te−Mo(2)	2.607(1)	Te−Fe(1)	2.743(2)
S(1)−Fe(1)	2.240(3)	S(2)−Fe(2)	2.247(3)
Te−Mo(1)	2.607(2)	Te−Fe(2)	2.712(2)
Mo(2)−S(1)	2.397(3)	Mo(2)−Fe(1)	2.851(2)
Mo(1)−S(2)	2.400(3)	Mo(1)−Fe(2)	2.860(2)
Mo(2)−Mo(1)	2.725(2)	Mo(2)−S(2)	2.402(4)
Mo(2)−Fe(2)	2.869(2)		

Mo(2)−Te−Mo(1)	63.0(1)	Mo(1)−Te−Fe(1)	65.1(1)
Mo(1)−Te−Fe(2)	65.0(1)	Te−Mo(2)−Mo(1)	58.5(1)
Mo(1)−Mo(2)−S(1)	55.5(1)	Mo(1)−Mo(2)−S(2)	55.4(1)
Te−Mo(2)−Fe(1)	60.1(1)	S(1)−Mo(2)−Fe(1)	49.6(1)
Te−Mo(2)−Fe(2)	59.1(1)	S(1)−Mo(2)−Fe(2)	114.7(1)
Fe(1)−Mo(2)−Fe(2)	111.7(1)	Te−Mo(1)−S(1)	98.0(1)
Te−Mo(1)−S(2)	97.8(1)	S(1)−Mo(1)−S(2)	80.6(1)
Mo(2)−Mo(1)−Fe(1)	61.1(1)	S(2)−Mo(1)−Fe(1)	114.2(1)
Mo(2)−Mo(1)−Fe(2)	61.8(1)	S(2)−Mo(1)−Fe(2)	49.6(1)
Mo(2)−Te−Fe(1)	64.3(1)	Mo(2)−Te−Fe(2)	65.3(1)
Fe(1)−Te−Fe(2)	120.4(1)	Te−Mo(2)−S(1)	98.2(1)
Te−Mo(2)−S(2)	97.7(1)	S(1)−Mo(2)−S(2)	80.6(1)
Mo(1)−Mo(2)−Fe(1)	62.2(1)	S(2)−Mo(2)−Fe(1)	115.2(1)
Mo(1)−Mo(2)−Fe(2)	61.4(1)	S(2)−Mo(2)−Fe(2)	49.5(1)
Te−Mo(2)−Mo(1)	58.5(1)	Mo(2)−Mo(1)−S(1)	55.3(1)
Mo(2)−Mo(1)−S(2)	55.5(1)	Te−Mo(1)−Fe(1)	59.7(1)
S(1)−Mo(1)−Fe(1)	49.2(1)	Te−Mo(1)−Fe(2)	59.3(1)
S(1)−Mo(1)−Fe(2)	114.8(1)	Fe(1)−Mo(1)−Fe(2)	111.1(1)
Mo(2)−S(1)−Mo(1)	69.2(1)	Mo(1)−S(1)−Fe(1)	76.6(1)
Mo(2)−S(2)−Mo(1)	69.1(1)	Mo(1)−S(2)−Fe(2)	75.9(1)
Mo(2)−Fe(1)−Mo(1)	56.8(1)	Mo(2)−Fe(1)−S(1)	54.6(1)
Te−Fe(2)−Mo(1)	55.7(1)	Te−Fe(2)−S(2)	98.7(1)
Mo(1)−Fe(2)−S(2)	54.5(1)	Te−Fe(1)−Mo(1)	55.2(1)
Te−Fe(1)−S(1)	98.3(1)	Mo(1)−Fe(1)−S(1)	54.2(1)
Te−Fe(2)−Mo(2)	55.6(1)	Mo(2)−Fe(2)−Mo(1)	56.8(1)
Mo(2)−Fe(2)−S(2)	54.4(1)		

Table 5. Selected Bond Lengths (Å) and Bond Angles (deg) for 4

Mo(1)−Mo(2)	3.129(1)	Mo(1)−Fe	2.794(1)
Mo(2)−Te	2.700(1)	Mo(1)−Te	2.700(1)
Mo(2)−Fe	2.830(1)	Te−Fe	2.515(1)

Mo(2)−Mo(1)−Te	54.6(1)	Te−Mo(1)−Fe	54.5(1)
Mo(1)−Mo(2)−Fe	55.6(1)	Mo(1)−Te−Mo(2)	70.8(1)
Mo(2)−Te−Fe	65.6(1)	Mo(1)−Fe−Te	60.9(1)
Mo(2)−Mo(1)−Fe	56.7(1)	Mo(1)−Mo(2)−Te	54.6(1)
Te−Mo(2)−Fe	54.0(1)	Mo(1)−Te−Fe	64.7(1)
Mo(1)−Fe−Mo(2)	67.6(1)	Mo(2)−Fe−Te	60.3(1)

Table 6. Selected Bond Lengths (Å) and Bond Angles (deg) for 6

Mo(1)−Mo(2)	2.783(1)	Mo(1)−S	2.620(2)
Mo(1)−Te	2.680(1)	Mo(1)−Fe(1)	2.928(2)
Mo(1)−Fe(2)	2.814(2)	Mo(2)−S	2.535(2)
Mo(2)−Te	2.800(2)	Mo(2)−Fe(1)	2.721(2)
Mo(2)−Fe(2)	2.672(2)	S−Fe(1)	2.217(3)
Te−Fe(2)	2.474(2)	Fe(1)−Fe(2)	2.545(2)
Mo(2)−Mo(1)−S	55.9(1)	S−Mo(1)−Te	117.4(1)
S−Mo(1)−Fe(1)	46.7(1)	Mo(2)−Mo(1)−Fe(2)	57.0(1)
Te−Mo(1)−Fe(2)	53.5(1)	Mo(1)−Mo(2)−Te	57.4(1)
Mo(1)−Mo(2)−Fe(1)	64.3(1)	Te−Mo(2)−Fe(1)	102.6(1)
S−Mo(2)−Fe(2)	98.2(1)	Fe(1)−Mo(2)−Fe(2)	56.3(1)
Mo(1)−S−Mo(2)	65.3(1)	Mo(2)−Mo(1)−Te	61.6(1)
Mo(2)−Mo(1)−Fe(1)	56.8(1)	Te−Mo(1)−Fe(1)	100.4(1)
S−Mo(1)−Fe(2)	92.8(1)	Fe(1)−Mo(1)−Fe(2)	52.6(1)
Mo(1)−Mo(2)−S	58.8(1)	S−Mo(2)−Te	116.1(1)
S−Mo(2)−Fe(1)	49.7(1)	Mo(1)−Mo(2)−Fe(2)	62.1(1)
Te−Mo(2)−Fe(2)	53.7(1)	Mo(2)−S−Fe(1)	69.5(1)
Mo(1)−Te−Fe(2)	66.1(1)	Mo(1)−Fe(1)−Mo(2)	58.9(1)
Mo(2)−Fe(1)−S	60.8(1)	Mo(2)−Fe(1)−Fe(2)	60.9(1)
Mo(1)−Fe(2)−Te	60.5(1)	Mo(1)−Fe(2)−Fe(1)	66.0(1)
Te−Fe(2)−Fe(1)	118.3(1)	Fe(2)−C(14)−O(14)	142.8(11)
Mo(1)−C(15)−O(15)	157.8(11)	Fe(1)−C(14)−O(14)	137.2(11)
Mo(1)−Te−Mo(2)	61.0(1)	Mo(2)−Te−Fe(2)	60.5(1)
Mo(1)−Fe(1)−S	59.3(1)	Mo(1)−Fe(1)−Fe(2)	61.4(1)
S−Fe(1)−Fe(2)	111.4(1)	Mo(1)−Fe(2)−Mo(2)	60.9(1)
Mo(2)−Fe(2)−Te	65.8(1)	Mo(2)−Fe(2)−Fe(1)	62.8(1)

Table 7. Selected Bond Lengths (Å) and Bond Angles (deg) for 8

Te−Mo(2)	2.603(2)	Te−Fe(1)	2.732(2)
Mo(2)−Mo(1)	2.739(2)	Mo(2)−Ss(2)	2.454(3)
Mo(2)−Fe(2)	2.877(3)	Mo(1)−Ss(1)	2.453(3)
Mo(1)−Fe(1)	2.886(3)	Ss(1)−Fe(1)	2.298(3)
Ss(2)−Fe(2)	2.292(3)	Te−Mo(1)	2.605(2)
Te−Fe(2)	2.710(3)	Mo(2)−Ss(1)	2.452(3)
Mo(2)−Fe(1)	2.860(3)	Mo(1)−Ss(2)	2.450(3)
Mo(1)−Fe(2)	2.873(3)		
Mo(2)−Te−Mo(1)	63.4(1)	Mo(1)−Te−Fe(1)	65.4(1)
Mo(1)−Te−Fe(2)	65.4(1)	Te−Mo(2)−Mo(1)	58.3(1)
Mo(1)−Mo(2)−Ss(1)	56.1(1)	Mo(1)−Mo(2)−Ss(2)	56.0(1)
Te−Mo(2)−Fe(1)	59.8(1)	Ss(1)−Mo(2)−Fe(1)	50.6(1)
Te−Mo(2)−Fe(2)	59.0(1)	Ss(1)−Mo(2)−Fe(2)	115.1(1)
Fe(1)−Mo(2)−Fe(2)	111.4(1)	Te−Mo(1)−Ss(1)	98.8(1)
Te−Mo(1)−Ss(2)	98.4(1)	Ss(1)−Mo(1)−Ss(2)	80.4(1)
Mo(2)−Mo(1)−Fe(1)	61.1(1)	Ss(2)−Mo(1)−Fe(1)	114.8(1)
Mo(2)−Mo(1)−Fe(2)	61.6(1)	Ss(2)−Mo(1)−Fe(2)	50.3(1)
Mo(2)−Te−Fe(1)	64.8(1)	Mo(2)−Te−Fe(2)	65.5(1)
Fe(1)−Te−Fe(2)	121.1(1)	Te−Mo(2)−Ss(1)	98.9(1)
Te−Mo(2)−Ss(2)	98.3(1)	Ss(1)−Mo(2)−Ss(2)	80.3(1)
Mo(1)−Mo(2)−Fe(1)	62.0(1)	Ss(2)−Mo(2)−Fe(1)	115.6(1)
Mo(1)−Mo(2)−Fe(2)	61.5(1)	Ss(2)−Mo(2)−Fe(2)	50.2(1)
Te−Mo(1)−Mo(2)	58.2(1)	Mo(2)−Mo(1)−Ss(1)	56.0(1)
Mo(2)−Mo(1)−Ss(2)	56.1(1)	Te−Mo(1)−Fe(1)	59.4(1)
Ss(1)−Mo(1)−Fe(1)	50.2(1)	Te−Mo(1)−Fe(2)	59.0(1)
Fe(1)−Mo(1)−Fe(2)	110.8(1)	Te−Fe(1)−Mo(2)	55.4(1)
Mo(2)−Fe(1)−Mo(1)	56.9(1)	Mo(2)−Fe(1)−Ss(1)	55.5(1)
Te−Fe(2)−Mo(1)	55.5(1)	Te−Fe(2)−Ss(2)	99.5(1)
Mo(1)−Fe(2)−Ss(2)	55.2(1)	Te−Fe(1)−Mo(1)	55.2(1)
Te−Fe(1)−Ss(1)	99.3(1)	Ss(1)−Mo(1)−Fe(2)	115.2(1)
Mo(1)−Fe(1)−Ss(1)	55.1(1)	Te−Fe(2)−Mo(2)	55.4(1)
Mo(2)−Fe(2)−Mo(1)	56.9(1)	Mo(2)−Fe(2)−Ss(2)	55.3(1)

determination of **7** has been carried out.[15] Compound **5** has been previously obtained from a metal exchange reaction involving the replacement of two $Co(CO)_3$ groups of $FeCo_2(\mu_3\text{-}S)(CO)_9$ with two $CpMo(CO)_2$ units.[16] Compounds **2**, **3**, and **8**, the mixed-chalcogenide analogues of **1**, and the previously reported $Cp_2Mo_2Fe_2(CO)_6(\mu_3\text{-}Se)_2(\mu_4\text{-}Se)$[17] all display a four-band carbonyl stretching pattern in their IR spectra. There is a lowering of the corresponding carbonyl stretching frequencies along the following combinations: SSeTe (**8**), S_2Te (**3**), STe_2 (**2**), and Te_3 (**1**). ^{125}Te NMR shifts are particularly sensitive to the bonding modes of the Te ligand. In the four related clusters **1**−**3** and **8**, the ^{125}Te NMR chemical shifts for the μ_4-Te and μ_3-Te ligands are well separated: δ >1600 ppm downfield with respect to $Te(CH_3)_2$ for the μ_4-Te ligand, and δ 727 and 698 ppm for the μ_3-Te atoms in **2** and **1**, respectively. The chemical shifts for the μ_3-Te atom in these compounds are upfield of the signals observed in the following compounds containing μ_3-Te ligands: $Fe_3(CO)_9(\mu_3\text{-}S)(\mu_3\text{-}Te)$, δ 828 ppm; $Fe_3(CO)_9(\mu_3\text{-}Se)(\mu_3\text{-}Te)$, δ 922 ppm.[18] There is a considerable difference between the chemical shifts observed for the μ_3-Te atom in **4**, δ 30 ppm, and for the μ_3-Te atoms in **6** and **7**, δ 1293 and 1386 ppm, respectively. The ^{77}Se NMR spectrum of **8** shows a signal at δ 659 ppm, which is slightly upfield of the signal at δ 679 ppm observed for $Fe_3(CO)_9(\mu_3\text{-}S)(\mu_3\text{-}Se)$. It is upfield by 119 and 208 ppm of the signals observed for $Fe_3(CO)_9(\mu_3\text{-}Se)_2$ and $Fe_3(CO)_9(\mu_3\text{-}Se)(\mu_3\text{-}Te)$, respectively.[19] It is also upfield of the signals observed for $CpCoFe_2(CO)_6(\mu_3\text{-}Se)_2$ (δ 796 ppm) and $CpCoFe_2(CO)_6(\mu_3\text{-}Se)(\mu_3\text{-}S)$ (δ 738 ppm).[10a] There is no significant difference observed in ^{13}C NMR chemical shifts for compounds **1**−**3** and **8**. The signal for the Cp carbon is observed in the range 85−92 ppm, whereas the signal for carbonyl carbon is observed in the range 213−214 ppm. Two signals for the Cp ring in the range δ 90−94 ppm, indicating the presence of nonequivalent Cp rings, are observed for compounds **6** and **7**; ^{1}H NMR also shows the presence of two nonequivalent Cp rings. Infrared spectra of compound **6** and **7** shows presence of bridging carbonyl groups. Chemical shifts in ^{1}H NMR spectra of compounds **1**−**3** and **8** show a downfield shift in the Cp signal when a lighter chalcogen atom is replaced by a heavier one.

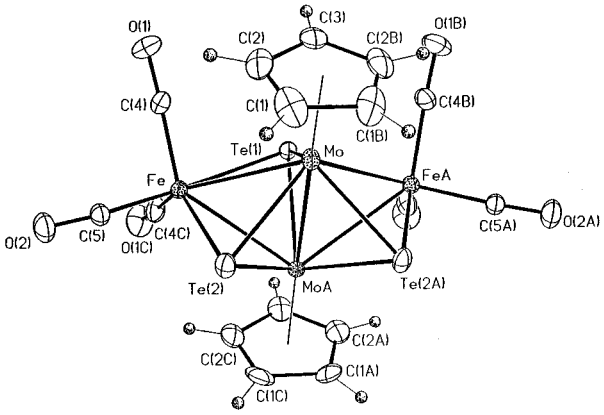

Figure 1. Molecular geometry and atom-labeling scheme for $Cp_2Mo_2Fe_2(\mu_4\text{-}Te)(\mu_3\text{-}Te)_2(CO)_6$ (**1**).

Molecular Structures of 1−3 and 8. Red crystals of **1**−**3** and black crystals of **8** were grown from hexane solution at −10 °C, and X-ray analyses were undertaken. Molecular structures of the four compounds **1**−**3** and **8** are shown in Figures 1−4, respectively. The four compounds are isostructural. The basic cluster geometry consists of two $FeMo_2$ triangular arrays with a common Mo_2 edge. In **1**, each plane has a μ_3-bonded

(15) Bogan, L. E.; Rauchfuss, T. B.; Rheingold, A. L. *J. Am. Chem. Soc.* **1985**, *107*, 3843.
(16) Richter, F.; Ronald, E.; Vahrenkamp, H. *Chem. Ber.* **1984**, *117*, 2429.
(17) Mathur, P.; Hossain, M. M.; Rheingold, A. L. *Organometallics* **1993**, *12*, 5029.
(18) Unpublished results for ^{125}Te NMR data: $Fe_3(CO)_9(\mu_3\text{-}S)(\mu_3\text{-}Te)$, δ 828; $Fe_3(CO)_9(\mu_3\text{-}Se)(\mu_3\text{-}Te)$, δ 922.
(19) Unpublished results for ^{77}Se NMR data: $Fe_3(CO)_9(\mu_3\text{-}S)(\mu_3\text{-}Se)$, δ 679; $Fe_3(CO)_9(\mu_3\text{-}Se)_2$, δ 778; $Fe_3(CO)_9(\mu_3\text{-}Se)(\mu_3\text{-}Te)$, δ 867.

Table 8. Spectroscopic Data for 1−8

compd	IR (ν, cm^{-1})	^{1}H NMR (δ, $CDCl_3$)	^{13}C NMR (δ, $CDCl_3$)	^{125}Te NMR (δ, $CDCl_3$)
$Cp_2Mo_2Fe_2Te_3(CO)_6$ (**1**)	2009 (w), 1992 (vs), 1950 (m), 1942 (m)[a]	4.6 (C_5H_5)	85 (C_5H_5), 214 (*C*O)	698 (μ_3-Te), 1675 (μ_4-Te)
$Cp_2Mo_2Fe_2STe_2(CO)_6$ (**2**)	2020 (w), 1998 (vs), 1955 (m), 1944 (m)[a]	4.8 (C_5H_5)	92 (C_5H_5), 214 (*C*O)	727 (μ_3-Te), 1676 (μ_4-Te)
$Cp_2Mo_2Fe_2S_2Te(CO)_6$ (**3**)	2021 (w), 2004 (vs), 1960 (m), 1946 (m)[a]	5.0 (C_5H_5)	92 (C_5H_5), 213 (*C*O)	1628 (μ_4-Te)
$Cp_2Mo_2FeTe(CO)_7$ (**4**)	2056 (w), 2019 (s), 1974 (m), 1949 (s), 1882 (br, w)[b]	5.2(C_5H_5)	93 (C_5H_5), 215 (*C*O)	30 (μ_3-Te)
$Cp_2Mo_2FeS(CO)_7$ (**5**)	2040 (s), 1985 (s), 1966 (m), 1899 (br, w), 1846 (br, w)[b]	5.3 (C_5H_5)	91 (C_5H_5), 212 (*C*O)	
$Cp_2Mo_2FeSTe(CO)_7$ (**6**)	2017 (s), 1989 (vs), 1957 (s), 1830 (br, m), 1735 (br, m), 1605 (m)[b]	5.5 (C_5H_5), 5.2 (C_5H_5)	92 (C_5H_5), 94 (C_5H_5), 212 (*C*O), 210 (*C*O), 207 (*C*O)	1293 (μ-Te)
$Cp_2Mo_2Fe_2Te_2(CO)_7$ (**7**)	2013 (vs), 1989 (s), 1952 (s), 1822 (br, m), 1639 (br, m), 1609 (m)[b]	5.4 (C_5H_5), 5.1 (C_5H_5)	90 (C_5H_5), 91 (C_5H_5), 211 (*C*O), 213 (*C*O)	1386 (μ_3-Te)
$Cp_2Mo_2Fe_2SSeTe(CO)_6$ (**8**)[c]	2024 (w), 2002 (vs), 1958 (m), 1949 (m)[a]	5.0 (C_5H_5)	90 (C_5H_5), 213 (*C*O)	1660 (μ_4-Te)

[a] Hexane solvent. [b] CH_2Cl_2 solvent. [c] ^{77}Se NMR data for **8** (δ, $CDCl_3$): 659 (μ_3-Se).

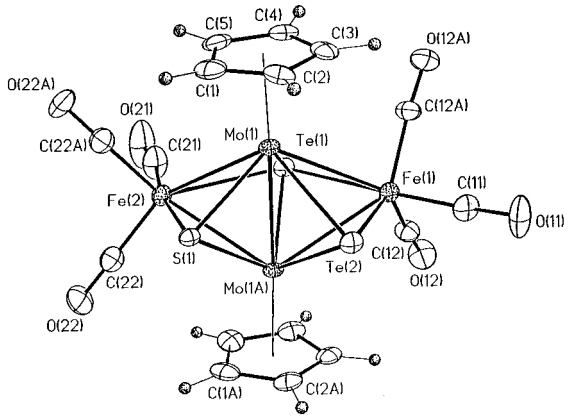

Figure 2. Molecular geometry and atom-labeling scheme for $Cp_2Mo_2Fe_2(\mu_4\text{-Te})(\mu_3\text{-Te})(\mu_3\text{-S})(CO)_6$ (**2**).

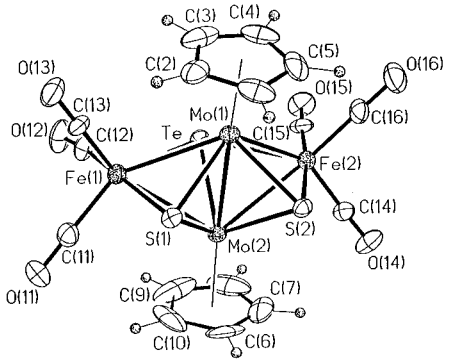

Figure 3. Molecular geometry and atom-labeling scheme for $Cp_2Mo_2Fe_2(\mu_4\text{-Te})(\mu_3\text{-S})_2(CO)_6$ (**3**).

Te atom above it. In compounds **2** and **8**, each $FeMo_2$ plane has a different μ_3-bonded chalcogen atom: in **2**, S and Te, and in **8**, S and Se. In compound **3**, the two Fe_2Mo planes are capped by μ_3-S ligands. In all four compounds, a third chalcogen ligand is present, a μ_4-Te atom, which is bonded to all four metal atoms. The geometry of the μ_4-Te ligand observed in these compounds is unusual; it is, however, similar to the μ_4-Se ligand in the related cluster $Cp_2Mo_2Fe_2(\mu_4\text{-Se})(\mu_3\text{-Se})_2(CO)_6$[17] and the large clusters $Co_9Se_{11}(PPh_3)_6$, $Ni_8Se_6(PPr_3)_4$, and $Ni_{34}Se_{22}(PPh_3)_{10}$.[20] It is also similar to the μ_4-S ligands in $Cp_2Mo_2(\mu_4\text{-S})(\mu_3\text{-S})_2Co_2(CO)_4$,[21] $Cp_4Cr_2Ni_2(\mu_4\text{-S})(\mu_3\text{-S})_2$,[22] $Ni_9(\mu_4\text{-S})_3(\mu_3\text{-S})_6(PEt_3)_6^{2+}$,[23] and $Mo_4(NO)_4(\mu\text{-}S_2)_5(\mu_4\text{-S})^{4-}$.[24]

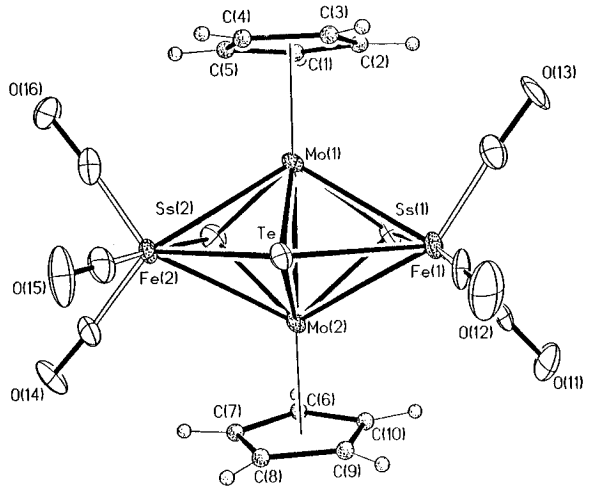

Figure 4. Molecular geometry and atom-labeling scheme for $Cp_2Mo_2Fe_2(\mu_4\text{-Te})(\mu_3\text{-S})(\mu_3\text{-Se})(CO)_6$ (**8**).

The Mo−Mo bond distance of 2.8172(12) Å in **1** is longer than the Mo−Mo bond distances in **2**, **3**, and **8** (2.7510(13), 2.725(2), and 2.730(2) Å, respectively), and the Mo−Mo bond distance of 2.743(2) Å in the Se_3 analogue $Cp_2Mo_2Fe_2(\mu_4\text{-Se})(\mu_3\text{-Se})_2(CO)_6$.[25] These distances are longer than the Mo−Mo bond distance of 2.624(2) Å observed in $(CH_3C_5H_4)_2Mo_2Fe_2(\mu_3\text{-S})_4(CO)_6$, which has a planar arrangement of the four metal atoms, but are slightly shorter than the Mo−Mo bond distances in other clusters which feature a Mo_2Fe_2 butterfly core structure: 2.821(1) Å in $Cp'Mo_2Fe_2(\mu_3\text{-S})_2(CO)_6(\mu\text{-CO})_2$ and 2.846(5) Å in $Cp_2Mo_2Fe_2(\mu_3\text{-S})_2(CO)_6(\mu\text{-CO})_2$.[11b] The metal−metal bond distances in **1**−**3** and **8** increase as the size of the μ_3-chalcogen atoms increases. Compound **1**, which has both the Mo_2Fe planes capped by Te ligands, has the longest Mo−Fe bond distance of the four compounds 2.9357(11) Å), and compound **3**, in which both Mo_2Fe planes are capped by S atoms, has the shortest Mo−Mo and Mo−Fe bond distances (2.725(2) and 2.865 Å (average respectively). In compound **2**, the Mo−Fe bonds which are associated with the μ_3-Te ligand are longer than the Mo−Fe bonds which are associated with the μ_3-S ligand (2.905 and 2.854 Å, respectively). The bond distance between the

(20) (a) Fenske, D.; Ohmer, J.; Hachbenei, J. *Angew. Chem., Int. Ed. Engl.* **1985**, *24*, 993. (b) Fenske, D.; Krautscheid, H.; Muller, M. *Angew. Chem., Int. Ed. Engl.* **1992**, *31*, 321.
(21) Curtis, M. D.; Williams, P. D. *Inorg. Chem.* **1983**, *22*, 2661.
(22) Passynskii, A. A.; Eremenko, I. L.; Ellert, O. G.; Novotortsev, V. M.; Rakitin, Y. V.; Kallinikov, V. T.; Shklover, V. E.; Struchkov, Y. T. *J. Organomet. Chem.* **1982**, *234*, 315.
(23) Ghilardi, C.; Midollini, S.; Sacconi, L. *J. Chem. Soc., Chem. Commun.* **1981**, 47.
(24) Muller, A.; Eltzner, W.; Mohan, N. *Angew. Chem., Int. Ed. Engl.* **1979**, *18*, 168.
(25) Cowans, B.; Noordik, J.; Rakowski-Dubois, M. *Organometallics* **1983**, *2*, 931.

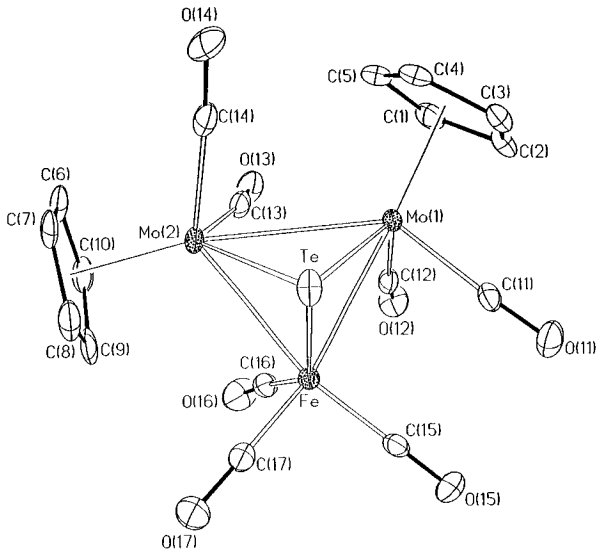

Figure 5. Molecular geometry and atom-labeling scheme for $Cp_2Mo_2Fe(\mu_3\text{-Te})(CO)_7$ (**4**).

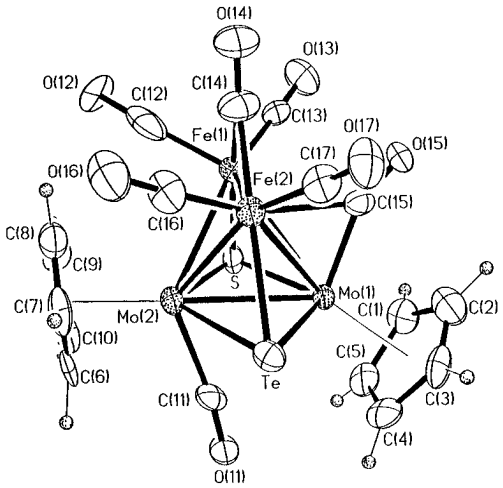

Figure 6. Molecular geometry and atom-labeling scheme for $Cp_2Mo_2Fe_2(\mu_3\text{-Te})(\mu_3\text{-S})(CO)_7$ (**6**).

μ_4-Te and the Mo atoms is shorter by ~0.03 Å than the bonds between the μ_3-Te atoms and the Mo atoms. The bonds between the Fe atoms and the μ_4-Te ligands are significantly longer (by ~0.3 Å) than the bonds between the Fe atoms and the μ_3-Te atoms. In compounds **1**, **3**, and **8**, the μ_4-Te ligand is symmetrically bridged between the two Mo atoms and the two Fe atoms; in contrast, in **2**, there is a slippage of the μ_4-Te ligand toward the Fe atom which is associated with the μ_3-Te atom (μ_4-Te to Fe(S), 2.849(2) Å; μ_4-Te to Fe(Te), 2.668(2) Å).

Molecular Structure of 4. Dark red crystals of **4** were grown by slow evaporation of its hexane/dichloromethane solution, and an X-ray analysis was undertaken. The molecular structure of **4** is depicted in Figure 5. The structure consists of a $FeMo_2Te$ tetrahedron. Each Mo atom possesses one Cp and two CO groups, and the Fe atom has three CO groups bonded to it. Its structure is similar to that of $Cp_2Mo_2Fe(\mu_3\text{-Se})(CO)_7$. The Mo−Mo distance of 3.129(1) Å is much longer than the Mo−Mo distances of 2.730(2)-2.817(1) Å in the trichalcogenide clusters **1**−**3** and **8** and 2.624(2) Å in $(MeCp)_2Mo_2Fe_2S_4(CO)_6$.[25] It is comparable with the Mo−Mo bond distance of 3.096(1) Å in the Se compound $Cp_2Mo_2Fe(\mu_3\text{-Se})(CO)_7$[12] and the average Mo−Mo bond distance of 3.116 Å in $Cp_3Mo_3(CO)_6(\mu_3$-As).[26] The average Fe−Mo bond distance of 2.812 Å in **4** is shorter than the Fe−Mo bond distances of 2.905 Å in $H(Cp)MoCoFe(CO)_8(\mu_3\text{-GeBu}^t)$,[27] 2.95 Å in $(MeCp)_2Mo_2Fe_2S_4(CO)_6$, and 2.9357 Å in **1** but similar to the average Fe−Mo bond distances of 2.835 Å in $Cp_2Mo_2Fe(\mu_3\text{-Se})(CO)_7$ and 2.847 Å in $Cp_2Mo_2Fe_2(\mu_4\text{-Se})(\mu_3\text{-Se})_2(CO)_6$. All other bond metricals of **4** are unexceptional.

Molecular Structure of 6. Black crystals of **6** were obtained from its hexane/dichloromethane solution at −10 °C, and an X-ray analysis was undertaken. The molecular structure of **6** is shown in Figure 6. The basic cluster geometry consists of a Mo_2Fe_2 tetrahedron with one Mo_2Fe face capped by a μ_3-Te atom and the other by a μ_3-S atom. Overall, the structure of **6** is similar to those of $Cp_2Mo_2Fe_2Te_2(CO)_7$[15] and $Cp_2Mo_2Fe_2Se_2(CO)_7$. One of the Mo atoms possesses a semitriply bridging CO ligand (Mo(1)−C(15)−O(15) = 157.8(11)°), similar to the ones in $Cp_2Mo_2Fe_2Te_2(CO)_7$ (Mo−C−O = 158.1(9)°) and $Cp_2Mo_2Fe_2Se_2(CO)_7$ (Mo−C−O = 159(3)°). Each Fe atom has two terminally bonded carbonyl groups, and one CO ligand bridges the Fe−Fe bond. The Fe−Fe bond distance of 2.545(2) Å is longer than the Fe−Fe bond distances observed for $Cp_2Mo_2Fe_2(CO)_7$ (2.433(2) Å) and $Cp_2Mo_2Fe_2Se_2(CO)_7$ (2.442(2) Å). The bridging C−O distance in **6** (C(14)−O(14) = 1.121(17 Å) is shorter than the bridging C−O distances of 1.191 Å in $Cp_2Mo_2Fe_2Te_2(CO)_7$ and 1.171(18) Å in $Cp_2Mo_2Fe_2Se_2(CO)_7$. The unbridged Mo atom has one terminally bonded CO group which points away from the cluster core.

Conclusion

In this paper, the synthesis of the mixed Fe−Mo trichalcogenide clusters **1**−**3** and **8** have been described. Formation of these compounds from the thermolysis reactions of chalcogens with **6** formally involves the cleavage of the Fe−Fe bond and loss of one carbonyl group of **6**. In the mixed-chalcogenide clusters **2**, **3**, and **8**, the μ_4-chalcogen is always the Te atom, and therefore, the mechanism must involve a shift of the Mo_2Fe face capping μ_3-Te in **6** to the μ_4 coordination seen in the trichalcogenide clusters, and the incoming chalcogen atom μ_3-caps one Mo_2Fe face. Formation of both **2** and **3** in the thermolysis reaction of **6** with Te powder suggests that some amount of cluster degradation occurs which liberates free S in the reaction medium. In competitive reactions between S and Te, S is more reactive toward **6**, leading to the formation of **3** in a higher yield than **2**. Although S must also be liberated during the thermolysis reaction of Se powder with **6**, formation of **3** was not observed in this reaction and **8** was isolated as the sole product. Further investigations are currently in progress to study in depth the contrasting reactivities of the chalcogen ligands in the mixed-chalcogenide clusters.

Acknowledgment. We are grateful to the Council of Scientific & Industrial Research, Government of India, for financial assistance to S.B.U.

Supporting Information Available: For 1−**4**, **6**, and **8**, tables of atomic coordinates, all bond lengths and bond angles, and anisotropic temperature factors (44 pages). Ordering information is given on any current masthead page.

OM950876S

(26) Blechsmitt, K.; Pfisterer, H.; Zhan, T.; Ziegler, M. L. *Angew. Chem., Int. Ed. Engl.* **1985**, *24*, 66.
(27) Gusbeth, P.; Vahrenkamp, H. *Chem. Ber.* **1985**, *118*, 1770.